Vortex interaction enhanced saturation number and caging effect in a superconducting film with a honeycomb array of nanoscale holes

M. L. Latimer,[1,2] G. R. Berdiyorov,[3] Z. L. Xiao,[1,2,*] W. K. Kwok,[1] and F. M. Peeters[3,†]
[1]*Materials Science Division, Argonne National Laboratory, Argonne, Illinois 60439, USA*
[2]*Department of Physics, Northern Illinois University, DeKalb, Illinois 60115, USA*
[3]*Departement Fysica, Universiteit Antwerpen, Groenenborgerlaan 171, B-2020 Antwerpen, Belgium*
(Received 26 November 2011; revised manuscript received 17 January 2012; published 26 January 2012)

The electrical transport properties of a MoGe thin film with a honeycomb array of nanoscale holes are investigated. The critical current of the system shows nonmatching anomalies as a function of applied magnetic field, enabling us to distinguish between multiquanta vortices trapped in the holes and interstitial vortices located between the holes. The number of vortices trapped in each hole is found to be larger than the saturation number predicted for an isolated hole and shows a nonlinear field dependence, leading to the caging effect as predicted from the Ginzburg-Landau (GL) theory. Our experimental results are supplemented by numerical simulations based on the GL theory.

DOI: 10.1103/PhysRevB.85.012505 PACS number(s): 74.50.+r, 74.45.+c, 74.78.Na

Subjected to an external drive, quantized magnetic flux lines (vortices) in type-II superconductors start to move, resulting in energy dissipation in the system. Their motion can be prevented by introducing pinning. It has been found that a periodic pinning landscape[1–11] leads to strong commensurability effects that appear when the number of vortices equals an integer (n) multiple of the number of pinning sites (i.e., at fields $H = nH_0$, with H_0 being the first matching field where the number of vortices equals the number of pins), resulting in peaks in, e.g., the critical current as a function of applied magnetic field. However, at larger magnetic fields the pinning centers become repulsive potentials for the incoming vortices, resulting in excess vortices, located preferentially at the interstitial sites between the pinning centers, forming different types of ordered vortex configurations.[12–16] The interstitial vortices can be highly mobile and lead to a strong reduction of the critical parameters of the system. In a superconducting film containing an array of holes the saturation number (i.e., the maximal number of pinned vortices per hole) is responsible for many phenomena and is a crucial quantity for the understanding of several superconducting properties. For example, it was found that the maximal number of vortices trapped by each hole in the absence of interstitial vortices controls the crossover between different pinning regimes[3,4] and helps to understand the magnetic field dependence of the magnetization of a patterned superconducting film.[3]

By considering the interaction between a single vortex and an isolated columnar defect of radius $R \ll \lambda$, Mkrtchyan and Shmidt[17] (see also Ref. 18 for the extension of their work) established that the saturation number is given by $n_{si} \cong R/2\xi(T)$, with $\xi(T)$ being the temperature-dependent coherence length. However, this expression can underestimate the saturation number for an array of holes where the interaction between vortices needs to be considered.[7,16] Indeed, careful analysis within the Ginzburg-Landau (GL) theory shows that[19] for an array of dense pinning centers the saturation number for a defect with a radius of the order of ξ becomes $n_{sa} \sim [R/\xi(T)]^2$ due to vortex-vortex interactions. Moreover, computer simulations reveal that interstitial vortices exert pressure on the pinning centers,[16,20,21] forcing additional vortices into the holes. Namely, interstitial vortices appear at lower magnetic fields, but as the vortex-vortex interaction increases at higher fields, vortices with more flux quanta start to form at the pinning sites.[16,20,21]

Experimentally, various techniques such as ac susceptibility measurements[7] and scanning Hall-probe microscopy[13] have been applied to determine the saturation number in a superconducting film containing an array of holes, and the values were found to be consistent with those predicted for an isolated pinning defect. On the other hand, scanning tunneling microscopy (STM)[22] and Bitter decoration[23] imagings show an increase of the vorticity of the multiquanta vortices in the hole after interstitial vortices were observed, revealing the effect of vortex-vortex interaction on the saturation number.[16,19] Though the pinning effect of a blind hole that allows the existence of multiple vortices of single-flux quantum may be different from that of a normal (through) hole having only one vortex with multiquanta, its saturation number seems also to depend on the vortex-vortex interaction: an increase in vortex number in blind holes after the appearance of interstitial vortices was also proposed to explain the reoccurrence of peaks at high integer matching fields observed in critical current versus magnetic field curves for superconducting films with square arrays of blind holes.[24]

Here we present results of transport measurements and computer simulations to address the saturation number issue for a superconducting film containing a regular array of holes. We study the transport properties of superconducting thin films with a honeycomb array of holes, which is constructed from a triangular array by removing 1/3 of the holes (see Fig. 1). In honeycomb pinning arrays, the interstitial regions are large, providing a unique platform to investigate the contribution of interstitial vortices to the trapping of vortices in the holes. As discussed below, in this system commensurate pinning enhancement may not occur at magnetic fields $H/H_0 = n$ but rather at $H/H_0 = n + 1/2$, which is clearly distinguished from the pinning phenomena of triangular and square arrangements of holes. In the latter cases the commensurate pinning effect is typically more pronounced at magnetic fields $H/H_0 = n$ than at $H/H_0 = n + 1/2$. This specific feature of the honeycomb

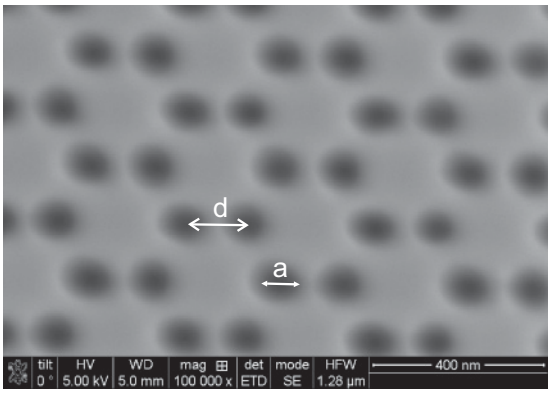

FIG. 1. Scanning electron microscopy image of the sample: a thin (20 nm) MoGe film with a honeycomb array of holes of diameter a separated by a distance d.

array helps us to distinguish between multiquanta vortex pinning in the holes and interstitial vortex pinning from an analysis of the transport data.

Superconducting systems with a honeycomb arrangement of pinning centers have attracted considerable interest in recent years. For example, extensive molecular dynamics simulations have been conducted in recent years,[21] which revealed remarkable variety of static and dynamic phenomena at integer and noninteger fillings. Experimental studies have also been performed recently, showing unusual features of such superconducting systems such as guided vortex motion.[25–28] In combination with computer simulations, we reveal that interstitial vortices appear once the saturation number n_{si} predicted for an isolated defect is exceeded. By further increasing the magnetic field, more vortices can indeed be trapped by each hole, with the maximal number approaching n_{sa}. We observed a stronger pinning at magnetic fields $H/H_0 = n + 1/2$ than at $H/H_0 = n$, where n is an integer and larger than n_{si}. This observation directly reveals the caging effect, i.e., the interstitial vortices are pinned by a confining caging potential exerted by vortices trapped in the holes.

Experiments were carried out on MoGe thin films, which are known for having extremely weak random pinning,[29] with a honeycomb array of holes of diameter a and spacing d (see Fig. 1). Films of thickness 20 nm were sputtered from a $Mo_{0.79}Ge_{0.21}$ alloy target onto a silicon substrate with 200-nm-thick oxide layer. Photolithography was used first to pattern the samples into a microbridge 50 μm wide. A honeycomb array of circular holes with desired diameters was fabricated through focused-ion-beam (FIB) milling (FEI Nova 600, 30-KeV Ga^+, 10–20-nm beam diameter) into the sections between the two voltage leads, which are 50 μm apart. Since the film is only 20 nm thick, through holes could be conveniently achieved. Transport measurements were carried out using a standard dc four-probe method with a physical property measurement system (PPMS-9, Quantum Design, Inc). We investigated samples with the same separation of holes $d = 150$ nm but for different diameters of the hole a. Here we present the results for samples with $a = 30$ nm (sample A) and 77 nm (sample B). The criterion $0.9R_n$, with R_n being the normal state resistance, gives us the zero-field critical temperatures T_{c0} of 5.3 and 5.7 K, respectively, for

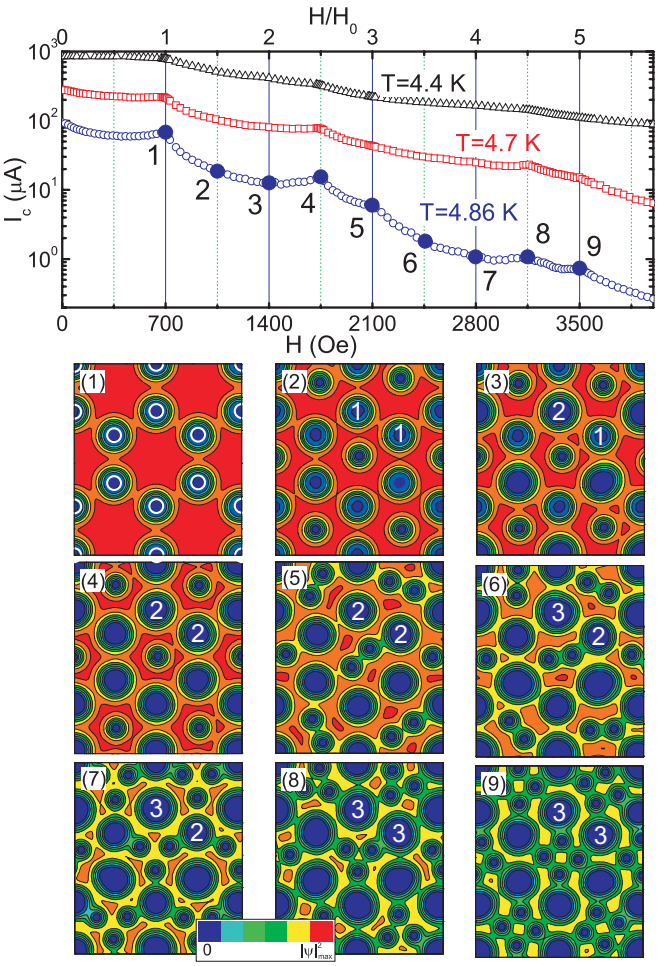

FIG. 2. (Color online) The critical current of a 20-nm-thick MoGe film with a honeycomb array of holes (diameter $a = 30$ nm and period $d = 150$ nm) as a function of perpendicular magnetic field at different temperatures. Panels 1–9 show contour-plots of the simulated ground state vortex configurations at zero applied current and at $T = 4.86$ K for the magnetic field values indicated in the main panel. White circles in panel 1 indicate the location of the holes, and white numbers show the number of vortices trapped in the holes.

samples A and B. Zero-temperature coherence length $\xi(0)$ and the penetration depth $\lambda(0)$ were estimated to be equal to 6 and 400 nm, respectively.

The magnetic field dependence of the critical current for sample A is presented in Fig. 2. As expected, commensurate pinning enhancement is observed at $H = H_0 = 700$ Oe when each hole gets one flux quantum. With further increasing the magnetic field, however, no commensurate pinning enhancement can be identified at $H = 2H_0$. Instead, a peak in the critical current can be clearly seen at $H = 2.5H_0$. As presented in Fig. 3 for sample B, which has bigger holes, a similar effect can also be identified at $H = 3H_0$ and $H = 3.5H_0$.

It is contrary to conventional behavior that the commensurate pinning enhancement is absent at an integer matching field and that it instead occurs at the following half-integer matching field. Experimental results similar to those observed in our sample B were reported for a superconducting Nb film with a honeycomb array of blind holes with a hole

spacing of 400 nm and a diameter of 270 nm, where the absence of the peak in the critical current at $H = 3H_0$ was attributed to a special arrangement of vortices in the holes and that the pinning enhancement at $H = 3.5H_0$ is due to a caging effect.[27] Interestingly, our sample B with through holes and the Nb films with blind holes have the same estimated saturation number $n_{si} = 2$ in the experimental temperature ranges. As presented below, however, our analysis indicates that vortices start to occupy the interstitial sites once n_{si} is reached. That is, the absence of the peak in the critical current at an integer matching field (e.g., $2H_0$ for sample A and $3H_0$ for sample B) is due to the high mobility of interstitial vortices. This provides a convenient way to identify vortex phases with and without interstitial vortices, enabling the determination of the maximal number of vortices trapped in the holes prior to the presence of interstitial vortices and of the increased vorticity of the multiquanta vortices at higher magnetic fields.

In order to visualize the vortex arrangements at various magnetic fields, we conducted simulations for the ground-state vortex configurations within the GL theory by numerically solving the time-dependent GL equation (in the zero electrostatic potential gauge):

$$\partial\psi/\partial t = (\nabla - i\mathbf{A})^2\psi + \left(1 - |\psi|^2\right)\psi + \chi(\mathbf{r},t). \qquad (1)$$

Here the distance is measured in units of the coherence length ξ, the vector potential $\mathbf{A}$ in units of $c\hbar/2e\xi$, and the order parameter ψ in units of $\sqrt{\alpha/\beta}$, with α and β being the GL coefficients. χ is the random force to simulate fluctuations.[30] We consider a very thin (thickness $t \ll \xi,\lambda$) superconducting sample with 90 holes of diameter a arranged in a honeycomb array of period d in the presence of a uniform perpendicular magnetic field H. Due to the small thickness of the sample we neglected demagnetization effects, i.e., the magnetic field inside the sample is equal to the applied one $\mathbf{A} = (-Hy/2, Hx/2, 0)$. Following the numerical approach of Ref. 30, we discretized Eq. (1) using the finite difference technique on a uniform two-dimensional (2D) Cartesian grid (with grid spacing 0.2ξ). A superconducting-vacuum boundary condition $(-i\nabla - \mathbf{A})\psi|_n$ is used at the sample edges and at the boundaries of the holes. Ground-state vortex configurations are obtained in field-cooled simulations starting from different random initial conditions for a given magnetic field. As demonstrated in Ref. 16 for a superconducting film containing a square array of holes, such simulated results reveal the representative vortex arrangements correlated with the observed critical currents, though the calculations were done in the absence of a drive.

We start by considering first sample A with small-size holes, $a = 30$ nm, so that only one vortex can be pinned by the holes at small magnetic fields. As illustrated in Fig. 2 , a peak observed at the first matching field $H_0 = 700$ Oe is due to the complete filling of the holes by vortices (see panel 1). I_c decreases with increasing magnetic field due to the appearance of interstitial vortices (panel 2). This is in spite of the fact that interstitial vortices tend to arrange into a triangular lattice, i.e., the overall vortex lattice is triangular at $H = 1.5H_0$ (panel 2). I_c decreases until $H = 2H_0$ (panel 3), after which a small increase in I_c is found due to the nonsymmetric pressure of the interstitial vortices on the pinned ones. By further increasing the field the critical current increases again, reaching a maximum at fractional matching field $H = 2.5H_0$ (point 4). This is due to the caging effect, as predicted previously.[16,31] The caging potential is created by the increased number of pinned vortices, which interact with the interstitial vortices repulsively. Our simulations show that the number of pinned vortices (in half of the holes) increases from 1 to 2 when the field increases from $H = 2H_0$ to $H = 2.5H_0$ (see panels 3 and 4; while the number of interstitial vortices remains the same), which is the ideal case for the caging effect. Although not pronounced, this effect can be observed at larger magnetic fields (see panels 7 and 8). In contrast, for example, at $H = 1.5H_0$ (see panel 2), there is only one pinned vortex in each hole, and they are not repulsive enough to cage the interstitial vortices, resulting in no enhancement in the critical current at that magnetic field. Such a caging effect originating from the increased number of pinned vortices in the holes was also observed in numerical simulations for a superconducting film containing a square array of holes: the critical current of the sample (open circles in Fig. 13 of Ref. 16) at the third matching field is larger than the one at the second matching field, though each cell has the

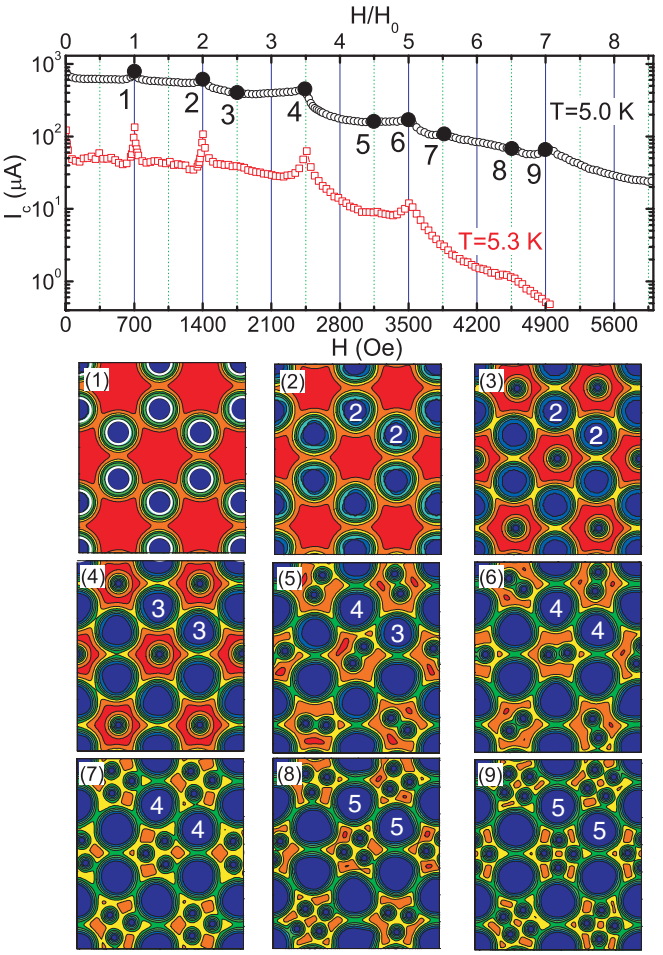

FIG. 3. (Color online) Critical current vs magnetic field for the sample with honeycomb arrangement of holes of diameter $a = 75$ nm and spacing $d = 150$ nm at two different temperatures. Panels 1–9 show the ground-state vortex configurations at the magnetic fields indicated in the main panel.

same (1) interstitial vortex at both fields. However, the number of vortices in each hole is one (1) and two (2) at the second and third matching fields, respectively. More pinned vortices in the holes at the third matching field create extra pinning potential for the interstitial vortices, thus increasing the critical current of the sample.

As predicted by both the saturation numbers n_{si} and n_{sa} for an isolated defect and for a defect array, respectively, larger holes should be able to accommodate more vortices. This in fact is confirmed by the experimental results in our sample B where the holes have a diameter $a = 77$ nm with an estimated saturation number $n_{si} = 2$. The results from our computer simulations, given in panels 1 and 2 of Fig. 3, indicate that all vortices are trapped in the holes at the field up to $2H_0$. At fields larger than the second matching field interstitial vortices appear, restoring the triangular arrangement of vortices (panel 3). By further increasing the field, extra vortices are pushed into the holes (panel 4), which shifts the peak in the critical current to a fractional matching field (see point 4 in the main panel). This is again the caging effect we discussed in the preceding paragraph. Such commensurability effects at half-integer matching fields are observed for vortex densities up to the seventh matching field with multiple pinned vortices at the interstitials (see panels 5–9).

Summarizing, we studied the transport properties of MoGe thin films with a honeycomb array of holes in the presence of a perpendicular magnetic field. With the help of numerical simulations within the GL theory, we were able to identify signatures that distinguish between multiquanta vortex pinning in the holes and interstitial vortex pinning. Our work shows that in a superconducting film containing a regular array of holes vortices will locate at the interstitial sites once the saturation number n_{si} predicted for an isolated hole is exceeded. However, the number of vortices trapped by the holes will continue to increase with increasing magnetic field and approach the saturation number n_{sa} predicted for a hole array. In the latter case the interstitial vortices will push additional vortices into the holes. This increase of the vorticity of the flux trapped in the holes and their interaction with interstitial vortices can induce novel phenomena, such as the caging effect, and result in an enhanced pinning strength at higher magnetic fields.

This work was supported by the Flemish Science Foundation (FWO-Vl) and the Belgian Science Policy (IAP) (theory) and by the US Department of Energy (DOE) Grant No. DE-FG02-06ER46334 (experiment). G.R.B. acknowledges an individual grant from FWO-Vl. W.K.K. acknowledges support from DOE BES under Contract No. DE-AC02-06CH11357, which also funds Argonne's Center for Nanoscale Materials (CNM), where the focused-ion-beam milling was performed. M.L.L was a recipient of the NIU/ANL Distinguished Graduate Fellowship.

*xiao@anl.gov
†francois.peeters@ua.ac.be

[1] P. Martinoli, Phys. Rev. B **17**, 1175 (1978).
[2] M. Baert *et al.*, Phys. Rev. Lett. **74**, 3269 (1995).
[3] V. V. Moshchalkov *et al.*, Phys. Rev. B **54**, 7385 (1996).
[4] V. V. Moshchalkov *et al.*, Phys. Rev. B **57**, 3615 (1998).
[5] V. Metlushko *et al.*, Phys. Rev. B **60**, R12585 (1999).
[6] A. V. Silhanek *et al.*, Phys. Rev. B **67**, 064502 (2003).
[7] A. V. Silhanek *et al.*, Phys. Rev. B **70**, 054515 (2004).
[8] A. V. Silhanek *et al.*, Phys. Rev. B **72**, 014507 (2005).
[9] U. Patel *et al.*, Phys. Rev. B **76**, 020508 (2007).
[10] A. V. Silhanek *et al.*, Phys. Rev. Lett. **104**, 017001 (2010).
[11] S. Avci *et al.*, Appl. Phys. Lett. **97**, 042511 (2010).
[12] K. Harada *et al.*, Science **274**, 1167 (1996).
[13] A. N. Grigorenko *et al.*, Phys. Rev. B **63**, 052504 (2001).
[14] C. Reichhardt *et al.*, Phys. Rev. B **57**, 7937 (1998).
[15] G. R. Berdiyorov *et al.*, Phys. Rev. Lett. **96**, 207001 (2006).
[16] G. R. Berdiyorov *et al.*, Phys. Rev. B **74**, 174512 (2006).
[17] G. S. Mkrtchyan and V. V. Shmidt, Sov. Phys. JETP **34**, 195 (1972).
[18] H. Nordborg and V. M. Vinokur, Phys. Rev. B **62**, 12408 (2000).
[19] M. M. Doria *et al.*, Phys. C **341–348**, 1199 (2000).
[20] M. M. Doria and G. F. Zebende, Phys. Rev. B **66**, 064519 (2002).
[21] C. Reichhardt and C. J. Olson Reichhardt, Phys. Rev. B **76**, 064523 (2007); Phys. Rev. Lett. **100**, 167002 (2008); Phys. Rev. B **78**, 224511 (2008); **79**, 134501 (2009); **81**, 024510 (2010).
[22] G. Karapetrov *et al.*, Phys. Rev. Lett. **95**, 167002 (2005).
[23] S. Rablen *et al.*, Phys. Rev. B **84**, 184520 (2011).
[24] R. Cao *et al.*, J. Appl. Phys. **109**, 083920 (2011).
[25] T. C. Wu *et al.*, J. Appl. Phys. **97**, 10B102 (2005).
[26] J. Cuppens *et al.*, J. Supercond. Novel Magn. **24**, 7 (2011).
[27] R. Cao *et al.*, J. Phys. Condens. Matter **21**, 075705 (2009).
[28] R. Cao *et al.*, J. Appl. Phys. **107**, 09E129 (2010).
[29] M. Liang *et al.*, Phys. Rev. B **82**, 064502 (2010).
[30] R. Kato *et al.*, Phys. Rev. B **47**, 8016 (1993).
[31] G. R. Berdiyorov *et al.*, Europhys. Lett. **74**, 493 (2006).